

On the performance of deterministic beamformers: A trade-off between array gain and attenuation



Martí Mañosas-Caballú*, José López Vicario, Gonzalo Seco-Granados

Department of Telecommunications and Systems Engineering, Universitat Autònoma de Barcelona, Bellaterra 08193, Spain

ARTICLE INFO

Article history:

Received 22 February 2013

Received in revised form

10 May 2013

Accepted 10 June 2013

Available online 17 June 2013

Keywords:

Beamforming

Array gain

Attenuation

Deterministic

ABSTRACT

It is customary to look over deterministic beamforming techniques as designs that offer a trade-off between mainlobe width and sidelobe level. In this work, we take into consideration that noise reduction and interference rejection are actually more useful metrics for the design of practical systems, and we present a novel analysis as a first step to understand the behavior and limitations of the deterministic beamformers from this system level perspective. The obtained results show that a trade-off between both metrics exists, and they illustrate some misconceptions about the traditionally assumed optimal designs. Finally, a method to approximately calculate the best attainable performance of any deterministic beamformer is presented.

© 2013 Elsevier B.V. All rights reserved.

1. Introduction

Beamforming is an array signal processing technique that provides a versatile form of spatial filtering. The existing beamforming techniques can be mainly classified into two groups [1]: *deterministic beamforming* and *data-dependent beamforming*. In the former, the designs aim to generate a fixed response for all possible scenarios, where sidelobe level and mainlobe width are typical performance metrics. In the latter, the designs depend on the statistics of the incoming data, where output signal-to-interference plus noise ratio (SINR) is a common performance metric.

Currently, the application requirements at a system level are usually present in terms of interference power and noise power at the output of the beamformer [2–4], and normally they cannot be understood simply as a single requirement on the interference-plus-noise power. These requirements can be alternatively expressed in terms of the beamformer's ability to mitigate the noise (*array gain*) and reject the interferences (*attenuation*), and they can be represented in a curve that relates both metrics. On the

other hand, each beamforming technique is inherently characterized by a performance curve containing the array gain and attenuation values that it can offer, each point corresponding to a specific design. A natural concern is then to accurately quantify the performance curves, since they allow us to know which designs can be eligible for the application of interest. Fig. 1a depicts this idea. This clearly casts doubts on the optimality of some commonly used beamforming performance metrics, and it shows that array gain and attenuation may be better metrics.

Recently, the authors of [4] studied the trade-off between array gain and attenuation of some data-dependent beamformers, and they proposed a new beamformer that allows the control of this trade-off. However, a similar study about deterministic beamformers is also necessary since unfortunately most data-dependent beamformers do not allow this control and they fail in some scenarios [1,5–7]. In contrast, deterministic beamformers constitute a robust [1,8,9] and simpler option to be implemented. Moreover, they offer adequate solutions when the desired signal and the interferences are known to be confined in different spatial regions, as in GNSS reference stations [3], radio telescopes for interferometry and the over-the-horizon radar.

In this work we shed some light on the relation between attenuation and array gain of the most relevant deterministic techniques. We compare their behavior and

* Corresponding author. Tel.: +34 93 581 40 30; fax: +34 93 581 40 31.

E-mail addresses: marti.manosas@uab.cat (M. Mañosas-Caballú),
jose.vicario@uab.cat (J. López Vicario),
gonzalo.seco@uab.cat (G. Seco-Granados).

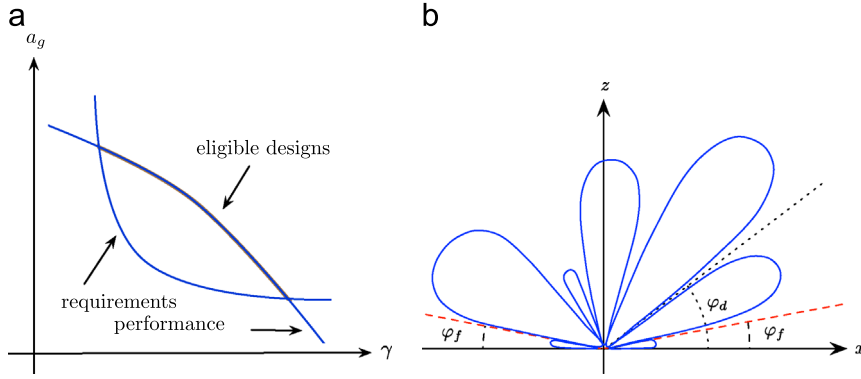


Fig. 1. (a) Example of the requirements and performance curves in terms of array gain (a_g) versus attenuation (γ). (b) Scenario of interest and example of a possible beam pattern.

limitations in a realistic scenario, and we show that the Dolph–Chebychev beamformer, which is usually adopted as the optimal solution to reject the signals coming from a given spatial sector, is not the best design from a system level perspective. In order to obtain a benchmark to evaluate the performance of any beamformer, we also present a method to approximately calculate the optimal performance curve.

2. Problem statement

Let us consider that an N -element uniform linear array receives $s(t)$, $m_1(t)$, \dots , $m_M(t)$ and $\mathbf{n}(t)$, which are the baseband representations of the desired signal, M interferences and additive white noise respectively. Assuming that the array narrow-band condition is fulfilled [1], the baseband equivalent of the beamformer output signal is

$$y(t) = \mathbf{w}^H \mathbf{v}(\theta_0) s(t) + \sum_{k=1}^M \mathbf{w}^H \mathbf{v}(\theta_k) m_k(t) + \mathbf{w}^H \mathbf{n}(t) \quad (1)$$

where $\mathbf{w} \in \mathbb{C}^N$ contains the beamforming weights, H denotes the conjugate transpose operation, $\mathbf{v}(\theta) \in \mathbb{C}^N$ is the steering vector at a given direction-of-arrival (DOA) θ , and $\theta_0, \theta_1, \dots, \theta_M$ are the DOAs of the desired signal and interferences respectively, defined as the arrival angles with respect to the array axis. Finally, $\mathbf{n}(t) \in \mathbb{C}^N$ contains the received noise at each element of the array.

In the applications of interest we cannot assume that the DOAs of the interferences are known. Instead, the interferences are assumed to arrive from elevations lower than a value φ_f , and we call this region *forbidden sector*. On the other hand, the desired signal arrives from an elevation higher than a value $\varphi_d > \varphi_f$, and we call this region *desired sector*. The remaining area is the *transition sector*. The elevations belonging to the forbidden sector correspond to $\theta \in [0, \varphi_f] \cup [\pi - \varphi_f, \pi]$, and for the desired one $\theta \in [\varphi_d, \pi - \varphi_d]$.

The aim of the beamformer is to find the weights \mathbf{w} that verify a particular requirements on the array response or beam pattern $\mathbf{w}^H \mathbf{v}(\theta)$. Fig. 1b shows a scheme of the described scenario and an example of a possible beam pattern. From all existing metrics related to \mathbf{w} , we are interested in the attenuation γ and the array gain a_g of the

corresponding beam pattern, defined as

$$\gamma^{-1} := \max\{|\mathbf{w}^H \mathbf{v}(\theta)|^2 / |\mathbf{w}^H \mathbf{v}(\theta_0)|^2 : \theta \in [0, \varphi_f] \cup [\pi - \varphi_f, \pi]\} \quad (2)$$

$$a_g := |\mathbf{w}^H \mathbf{v}(\theta_0)|^2 / |\mathbf{w}^H \mathbf{w}| \quad (3)$$

Note that the attenuation definition is consistent with the worst-case requirements of the considered applications, and the noise definition considers the special case of spatial white noise and identical noise spectra at each sensor [1].

The goal of the paper is then to study the relation between γ and a_g of the current deterministic beamformers for linear arrays and find an optimal performance curve to obtain a benchmark that let us evaluate their performance. The inter-element spacing of the array is chosen to be half wavelength through all the paper since the corresponding beam pattern presents the best resolution without ambiguity.

3. Array gain versus attenuation trade-off

3.1. Deterministic beamforming techniques

We discuss here how to adapt the existing deterministic techniques to our scenario. The first step is to select those methods in which either a_g or γ can be modified deliberately by the designer. This is only the case of the Main Response Axis (MRA) methods [1], which assure an accurate control of the sidelobe level.

The MRA methods mainly comprise the Spectral Weighting (SW) and the Minimum Beamwidth for Specified Sidelobe Level (MBSSL) approaches, which present a well known trade-off between sidelobe level and mainlobe width or beamwidth. Concretely, the MBSSL methods optimize the beamwidth for a given maximum level of sidelobes, and the Dolph–Chebychev is the best known representative because it has constant level of sidelobes. Furthermore, both approaches are characterized by having non-increasing sidelobes. This leads to a methodology of design based on building a spatial filter with pass-band given by the mainlobe and stop-band given by the sidelobes. In our scenario, the pass-band is located in the desired sector and the stop-band corresponds to the forbidden sector. The mainlobe is placed in the desired

direction θ_0 by means of *array steering* [1] since the mainlobe of all the MRA methods is located at $\theta_0 = \pi/2$ by default, and the first sidelobe level is meant to determine a lower-bound on the attainable attenuation.

Finally, note that this methodology of design may imply that a portion of the mainlobe is present in the forbidden sector because the closer to the endfire ($\theta = 0$ or π) the mainlobe is, the wider the beamwidth. Then, as γ is determined by the maximum value of sidelobes and mainlobe inside the forbidden sector, the mainlobe can reduce the attainable attenuation if it exceeds the sidelobe level. As a result, and being consistent with the considered worst case requirements, it is mandatory to focus on the designs where the DOA of $s(t)$ is close to the forbidden sector. Other cases are not so restrictive.

3.2. Trade-off analysis

We start by noting that the value of γ is generally improved by decreasing the sidelobes level. However, this generally widens the mainlobe. Thus, a situation may be attained where the mainlobe is present in the forbidden sector with a value that exceeds the sidelobes. As a result, each MRA technique has a maximum value of attenuation ϵ that is not possible to exceed, i.e. $\epsilon = \max \gamma$. We call it *maximum-attenuation design*, and it is achieved when the first sidelobe level equals the maximum mainlobe value inside the forbidden sector.

Without loss of generality, we can consider that our beam patterns are normalized with respect to the LOSS response, so ϵ corresponds to a minimum sidelobe level $1/\sqrt{\epsilon}$. In the case of the Dolph–Chebychev approach, it is possible to analytically deduce a formula for ϵ through simple algebraic manipulations on the beam pattern of the Dolph–Chebychev beamformer, whose basic formulation can be obtained from [1]

$$\epsilon = \cosh^2((N-1) \operatorname{sech}^{-1} \cos(\pi\rho/2)) \quad N \geq 2 \quad (4)$$

where $\rho = \cos(\varphi_f) - \cos(\varphi_d)$. In the case of the SW methods, the value of ϵ corresponds to the largest solution of

$$\sqrt{\epsilon}^{-1} = |\mathbf{w}(\epsilon)^H \mathbf{v}(\cos^{-1}\rho)| \quad \epsilon > 0 \quad (5)$$

where we use $\mathbf{w}(\epsilon)$ to emphasize that \mathbf{w} depends on the designed sidelobe level $1/\sqrt{\epsilon}$ through a MRA design parameter. Eq. (5) imposes that the value of the mainlobe at φ_f is equal to the first sidelobe level. Then, in practice one can obtain an approximate solution via beam pattern plots: increasing/decreasing the first sidelobe level until it equals the mainlobe value at φ_f . Analogously, an accurate solution of ϵ can be easily obtained from (5) via the bisection method.

As shown in (4) and (5), ϵ does not only depend on the particular design \mathbf{w} , but also on the value of N . Fig. 2 shows the minimum number of antennas N_{\min} needed to obtain a given value of ϵ . We can see that N_{\min} is a monotonically increasing function of ϵ . The reason is that an increase of ϵ requires a decrease of the beamwidth, which is achieved by increasing N . Note that the plot also shows that the SW methods can be classified into two groups [1]. On one hand, Hamming and Blackman–Harris, do not allow us to vary the sidelobe level deliberately, and they are

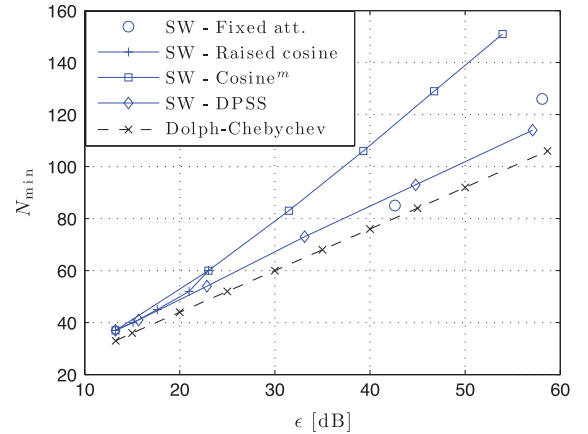


Fig. 2. Minimum number of antennas N_{\min} for achieving an attenuation ϵ . Scenario with $\varphi_f = 10^\circ$ and $\varphi_d = 20^\circ$.

represented as fixed attenuation points. On the other hand, Dolph–Chebychev, Raised Cosine, Cosine^m and Discrete Prolate Spheroidal Sequences (DPSS), allow us to increase or decrease the sidelobe level through a design parameter.

Finally, we analyze the points (a_g, γ) that an MRA method offers when varying the design parameter for a given value of N . This gives a curve for each value of N . Note first that if the designed sidelobes are higher or equal than $1/\sqrt{\epsilon}$, then γ is determined by the sidelobes level. However, when the designed sidelobes are lower than $1/\sqrt{\epsilon}$, then γ is determined by the mainlobe. Thus, two different designs may exist that produce the same γ . As each design corresponds to a different beamformer, a priori it has different values of a_g . The result is that some values of γ can be paired with two different values of a_g , except when $\gamma = \epsilon$. In fact, all simulated methods present an upper and lower curves ending at a common point with attenuation ϵ . In order to show only the most meaningful designs, we do not represent here the lower curve. Fig. 3 shows the upper curves obtained for the DPSS and Dolph–Chebychev methods.

3.3. Discussion

First note that, as the SW methods have decreasing sidelobes, there are sidelobes that are lower than the first sidelobe. But, as some of them are outside the forbidden region, they are not effectively used to attenuate interferences. In contrast, the Dolph–Chebychev approach offers a constant level of sidelobes, which is a less restrictive way of using the degrees of freedom of \mathbf{w} to increase γ , as corroborated by the results in Fig. 2. This advantage partially clarifies why the Dolph–Chebychev is usually adopted as the optimal solution to attenuate the signals coming from a given spatial sector. However, the Dolph–Chebychev method does not enjoy the same advantage in terms of a_g . For instance, Fig. 3 shows that for $N=40$ the SW techniques present the best values of a_g .

Second note that Fig. 3 shows that there exists a clear trade-off between a_g and γ . The SW methods present the best a_g when high sidelobes γ are used. This is due to both the narrow mainlobe of the beam patterns and the high filtration

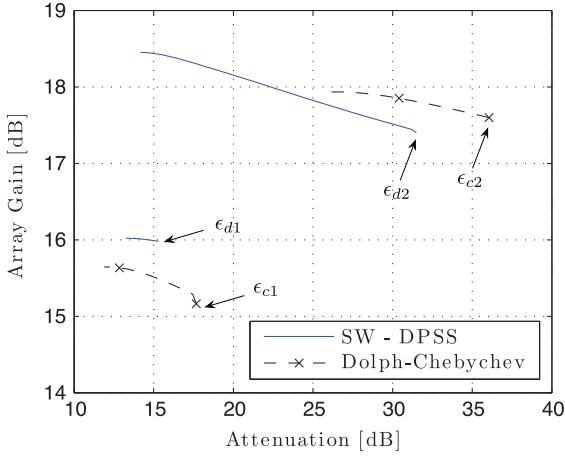


Fig. 3. Array gain versus attenuation for the DPSS and the Dolph-Chebyshev techniques. $N=40$ (lower curves) and $N=70$ (upper curves). The maximum-attenuation design values are $\epsilon_{d1} \approx 15.3$ dB, $\epsilon_{d2} \approx 31.5$ dB, $\epsilon_{c1} \approx 17.7$ dB and $\epsilon_{c2} \approx 36$ dB. Scenario with $\varphi_f = 10^\circ$ and $\varphi_d = 20^\circ$.

of the noise for low elevations. Then, when the designed sidelobes are lower, γ increases up to ϵ . But the mainlobe width increases and the higher noise reduction for low elevations does not compensate the incoming noise from the mainlobe, so a_g decreases. In contrast, in the case of the Dolph-Chebyshev, the noise is poorly mitigated in all the visible region for high sidelobes since the same low attenuation is applied for all the sidelobes, so a_g is low. Then, a_g is improved when the sidelobes are decreased, although the represented values are obtained once the sidelobes go under $1/\sqrt{\epsilon}$, so the attenuation decreases.

4. Optimal performance curve

We work out the values of the Optimal Performance Curve (OPC) from the solution of an iterative algorithm. Our goal is to solve

$$\begin{aligned} \max_{\mathbf{w}} \quad & |\mathbf{w}^H \mathbf{a}|^2 / |\mathbf{w}^H \mathbf{w}| \\ \text{s.t.} \quad & |\mathbf{w}^H \mathbf{v}(\theta)| / |\mathbf{w}^H \mathbf{a}| \leq \beta \quad \theta \in [0, \varphi_f] \cup [\pi - \varphi_f, \pi] \end{aligned} \quad (6)$$

where $\mathbf{a} := \mathbf{v}(\theta_0)$ to abbreviate and, without loss of generality, we can consider that $\mathbf{w}^H \mathbf{a} = 1$. Note that (6) maximizes a_g for a given attenuation $\gamma = \beta^2$, so its solution determines the optimal trade-off between a_g and γ . However, as this solution is very difficult to obtain (if possible at all), we present below an approximate solution by means of a modified version of the iterative algorithm presented in [10]. Although an analytical proof of the convergence of the proposed iterative algorithm to the approximate solution is not available, the results obtained in [10] and our extensive simulations have shown that in practice this is always the case as long as the constraint in (6) does not make the problem unfeasible. Note that in the considered scenarios a mathematical proof of the convergence is not really necessary since it can be just checked through simulations before using the weights for their final purpose.

The algorithm starts by creating a distortionless beamformer with maximum array gain, i.e. $\mathbf{w}_0 = \text{argmin } \mathbf{w}^H \mathbf{w}$

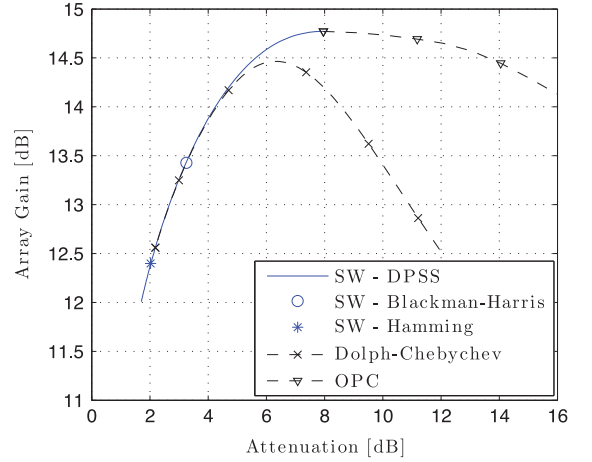


Fig. 4. Array gain versus attenuation for several MRA deterministic techniques and the OPC. $N=30$. Scenario with $\varphi_f = 10^\circ$ and $\varphi_d = 20^\circ$.

subject to $\mathbf{w}^H \mathbf{a} = 1$, whose solution is $\mathbf{w}_0 = (\mathbf{a}^H \mathbf{a})^{-1} \mathbf{a}$. Second, the algorithm iteratively updates the weights as $\mathbf{w}_{n+1} = \mathbf{w}_n + \Delta \mathbf{w}_n$ until the sidelobes do not exceed the desired level β in the forbidden sector. For a given value of $n \in \mathbb{N}$, $\Delta \mathbf{w}_n$ comes from

$$\begin{aligned} \min_{\Delta \mathbf{w}_n} \quad & (\mathbf{w}_n + \Delta \mathbf{w}_n)^H (\mathbf{w}_n + \Delta \mathbf{w}_n) \\ \text{s.t.} \quad & \Delta \mathbf{w}_n^H \mathbf{a} = 0 \\ & \Delta \mathbf{w}_n^H \mathbf{v}(\phi_{n,k}) = f_{n,k} \quad k = 1, \dots, K_n \end{aligned} \quad (7)$$

where $\phi_{n,k}$ is the direction of the k -th sidelobe of \mathbf{w}_n that exceeds β in the forbidden sector, K_n is the number of sidelobes that exceed β and $f_{n,k}$ is the value that we assign to the beam pattern of $\Delta \mathbf{w}_n$ in the direction $\phi_{n,k}$.

The goal of (7) is twofold. On one hand, using the new objective function and the constraint $\Delta \mathbf{w}_n^H \mathbf{a} = 0$, the maximization of the array gain of \mathbf{w}_{n+1} and the constraint $\mathbf{w}_{n+1}^H \mathbf{a} = 1$ are maintained. On the other hand, using the second constraint with $f_{n,k} := (\beta - |c_{n,k}|)c_{n,k}/|c_{n,k}|$ and defining $c_{n,k}$ as the value of the beam pattern of \mathbf{w}_n at $\phi_{n,k}$, the level of the selected sidelobes that exceed β is forced to be equal to β . In the case that $K_n > N-1$, only the highest $N-1$ sidelobes are considered, hence prioritizing the directions that exceed the sidelobe threshold in a greatest extent. Note that, assuming that convergence holds, $K_n \leq N-1$ must be verified from some iteration on. The solution of (7) is $\Delta \mathbf{w}_n = \mathbf{C}_n (\mathbf{C}_n^H \mathbf{C}_n)^{-1} \mathbf{g}_n - \mathbf{P}_{\mathbf{C}_n}^\perp \mathbf{w}_n$, where $\mathbf{C}_n = [\mathbf{a}, \mathbf{v}(\phi_{n,1}), \dots, \mathbf{v}(\phi_{n,K_n})]$, $\mathbf{g}_n = [0, f_{n,1}, \dots, f_{n,K_n}]^H$ and $\mathbf{P}_{\mathbf{C}_n}^\perp$ is the projection matrix onto the space orthogonal to the column space of \mathbf{C}_n .

Fig. 4 plots the OPC and the performance curves of the most representative MRA methods for $N=30$. As it is clearly shown, the OPC outperforms these deterministic designs, so it sets a reference to visualize how far they are from the optimal one. In addition, an interesting feature is observed when the OPC beam patterns are plotted: they present decreasing sidelobes outside the forbidden sector and approximately constant sidelobes in the forbidden sector. This is an intermediate behavior between those of the SW and the Dolph-Chebyshev and coincides with the fact that it may optimize the studied trade-off.

5. Conclusion

In this work we have presented a novel performance analysis of deterministic beamformers applied in a scenario with interferences coming from low elevations. We have argued that the well known trade-off between sidelobe level and mainlobe width is not useful to carry out performance assessment and design at system level. Therefore, we have considered the attenuation and the array gain as a parameters of interest, and we have analyzed the most outstanding deterministic techniques showing that a trade-off between both metrics exists. Finally, we have presented a method to approximately calculate the performance that defines the best possible trade-off and delimit the region of eligible designs. The corresponding beam patterns strike a balance between some aspects found in the Spectral Weighting techniques and others found in the Dolph–Chebychev.

References

- [1] H.L. Van Trees, *Optimum Array Processing. Detection, Estimation, and Modulation Theory. Part IV*, 1st edition, Wiley-Interscience, 2002.
- [2] J. Riba, J. Goldberg, G. Vazquez, Robust beamforming for interference rejection in mobile communications, *IEEE Transactions on Signal Processing* 45 (1997) 271–275.
- [3] J.L. Vicario, F. Antreich, M. Barcelo, N. Basta, J. Cebrian, M. Cuntz, O. Gago, L. Gonzales, V. Heckler, C. Lavin, M. Manosas-Caballú, J. Picanyol, G. Seco-Granados, M. Sgammini, F. Amarillo, ADIBEAM: Adaptive digital beamforming for Galileo reference ground stations, in: *Proceedings of ION GNSS*, 2010, Portland, OR, pp. 172–184.
- [4] M. Souden, J. Benesty, S. Affes, A study of the LCMV and MVDR noise reduction filters, *IEEE Transactions on Signal Processing* 58 (2010) 4925–4935.
- [5] Y. Bresler, V. Reddy, T. Kailath, Optimum beamforming for coherent signal and interferences, *IEEE Transactions on Acoustics Speech and Signal Processing* 36 (1988) 833–843.
- [6] S. Pillai, B. Kwon, Forward/backward spatial smoothing techniques for coherent signal identification, *IEEE Transactions on Acoustics Speech and Signal Processing* 37 (1989) 8–15.
- [7] G. Seco-Granados, J.A. Fernandez-Rubio, C. Fernandez-Prades, ML estimator and hybrid beamformer for multipath and interference mitigation in GNSS receivers, *IEEE Transactions on Signal Processing* 53 (2005) 1194–1208.
- [8] K.M. Buckley, L. Griffiths, Design of deterministic beamformers for arbitrarily configured arrays, in: *Proceedings of the IEEE ICASSP*, 1987, Minneapolis, MN, pp. 1995–1998.
- [9] C.-Y. Tseng, L.J. Griffiths, An iterative approach for deterministic beamformer design, in: *Proceedings of the Conference on Communication Computing and Signal Processing*, 1989, Victoria, BC, Canada, pp. 439–442.
- [10] C.-Y. Tseng, L. Griffiths, A simple algorithm to achieve desired patterns for arbitrary arrays, *IEEE Transactions on Signal Processing* 40 (1992) 2737–2746.